Biol Cybern (2006) 94: 483–499
DOI 10.1007/s00422-006-0061-0

ORIGINAL PAPER

Biological Cybernetics

H.R. Rabie · J. Rong · M.I. Glavinović

Monte Carlo simulation of release of vesicular content in neuroendocrine cells

Received: 18 October 2005 / Accepted 15 February 2006 / Published online: 21 March 2006

Abstract The release of transmitter from the vesicle, its diffusion through the fusion pore, and the cleft and its interaction with the carbon electrode were simulated using the Monte Carlo method. According to the simulation the transmitter release is largely determined by geometric factors – the ratio of the fusion pore cross-sectional and vesicular areas, if the diffusion constant is as in the aqueous solution – but the speed of transmitter dissociation from the gel matrix plays an important role during the rise phase of release. Transmitter is not depleted near the entrance to the fusion pore and there is no cleft-to-vesicle feedback, but the depletion becomes evident if the diffusion constant is reduced, especially if the pore is wide. In general, the time course of amperometric currents closely resembles the time course of the simulated transmitter concentration in the cleft and the time course of release. Surprisingly, even a tenfold change of the electrode efficiency has only a marginal effect on the amplitude or the time course of amperometric currents. Greater electrode efficiency however lowers the cleft concentration, but only if the cleft is narrow. As the cleft widens the current amplitudes diminish and rise times lengthen, but the decay times are less affected. Moreover, the amplitude dependence of the rise and decay times becomes steeper as the cleft widens and/or as the release kinetics slows. Finally, lower diffusion constant of transmitter in the narrow cleft does not further prolong the amperometric currents, whose slow time course reflects slow release kinetics.

Keywords Monte Carlo simulation · Gel storage · Amperometry · Diffusion · Catecholamine · Electrolysis

H.R. Rabie
Departments of Applied Chemical and Biological Sciences,
Ryerson Polytechnic University, Toronto, ON, Canada

J. Rong
Department of Computer Science, McGill University, Montreal,
QC, Canada

M.I. Glavinović (✉)
Department of Physiology, McGill University,
3655 Sir William Osler Promenade,
Montreal, Canada P.Q. H3G 1Y6
E-mail: mladen.glavinovic@mcgill.ca
Tel.: +514-398-6002
Fax: +514-398-7452

1 Introduction

Catecholamines have been found in a wide range of tissues and affect many physiological processes. Release of adrenaline and noradrenaline produced by a medullary discharge as part of the 'fight or flight' responses, or generally due to the stress conditions, leads to symptoms associated with anxiety. In the central nervous system the catecholamines (dopamine and noradrenaline) influence the prefrontal cortex working memory function and generally cognitive functions and its dysregulation is related to schizophrenia (Brozoski et al. 1979; Tanaka 2005). Moreover dopamine takes part in ischemia-induced neuronal damage (Saulle et al., 2002), and had also been extensively implicated in the mechanism of drug addiction (Di Chiara et al., 2004). Finally loss of dopamine negatively affects the nerves and muscles controlling movement and coordination, resulting in the symptoms characteristic of Parkinson's disease (Frucht, 2004).

Release of catecholamines (adrenaline, noradrenaline and dopamine) was first detected amperometrically from large dense core vesicles in chromaffin cells (which are neuroendocrine cells found in the medulla of the adrenal gland and in other ganglia of the sympathetic nervous system and which derive from the embryonic neural crest), and subsequently from small synaptic vesicles in the central nervous system (Wightman et al. 1991; Schroeder et al. 1994; Walker et al. 1996; Aspinwall et al. 1997; Anderson et al. 1999, Sulzer and Pothos 2000). Cyclic voltametry in the central nervous system has shown that dopamine diffuses beyond the confines of the synapse into the extracellular space (Garris et al. 1994), and its action is characterized by long delays (Di Chiara et al. 2004).

Understanding the factors determining the amplitude and time course of the basic unit of release – the unitary quantal

event – in synapses and neuro-endocrine cells is of fundamental importance. Amperometric recordings of the unitary quantal events have revealed that the time course of release from neuro-endocrine cells is often much longer, and that the quantal size, amplitude and the time course are much more variable than at either central or peripheral synapses (Wightman et al. 1991; Walker et al. 1996; Aspinwall et al. 1997; Amatore et al. 2000; Kebir et al. 2005). Biochemical evidence suggests that the catecholamines are stored at high concentrations, but in an osmotically inactive form, on a matrix of chromogranin A, and their release occurs through a process of dimerization of chromogranin A (Uvnas and Aborg 1989; Kelly 1993; Yoo and Lewis 1993). It was thus suggested that a slower release is due to the storage mechanism of catecholamines (Schroeder et al. 1994). However, the release will also be slower and more variable because the adrenaline or noradrenaline containing vesicles are considerably larger and their size more variable than synaptic vesicles, peripheral or central (Eccles and Jaeger 1958; Coupland 1968; Schikorski and Stevens 1997; Glavinović et al. 1998; Karunanithi et al. 2002; Tang et al. 2005). The amperometric currents may also be slower if the diffusion constant of catecholamines in the cleft near the membrane is lower due to its reversible binding to the cell membrane (Hafez et al. 2005), although such a reversible binding with the vesicular and fusion pore membrane would also slow the release kinetics. Recording conditions may be an additional factor. Greater separation between the secretory cell and the electrode (cleft width) reduces the amplitude and lengthens the duration of the amperometric currents (Wightman et al. 1991), but how much the changes of the efficiency of the carbon fiber to oxidize the released catecholamines will change the amplitude and the time course of the amperometric currents is not known.

In order to better understand how the vesicular size and its variability, the nature of transmitter storage, properties of the fusion pore, the transmitter diffusion in the cleft or the efficiency of electrolysis at the carbon filament surface affect the amplitude and the time course of amperometric currents we simulated the release of vesicular content using the Monte Carlo method (Glavinović 1999). The intravesicular transmitter concentration and the fusion pore dimensions were as reported in literature (Coupland 1968; Winkler et al. 1986; Spruce et al. 1990; Monck and Fernandez 1992; Khanin et al. 1994; Finnegan et al. 1996; Glavinović 1999; Anderson et al. 1999; Jena et al. 2003), whilst the recording electrode – secretory cell distance and the level of electrolysis varied over a wide range. A preliminary account has appeared (Glavinović and Rabie, 1997).

2 Materials and methods

2.1 Theory

The release of vesicular content was simulated using the Monte Carlo method, which is highly suitable for studying diffusion in systems having complex geometry (Wahl et al. 1996). The transmitter molecules in the vesicle (simulated as a sphere) were either all initially bound to a gel matrix, or were all free. Figure 6a. shows a schematic diagram (approximately to scale) of the vesicle connected through the fusion pore (simulated as a cylinder) to the plasma membrane, and releasing its contents into the space separating it from the carbon electrode (cleft). The plasma membrane and the recording electrode were simulated as two parallel plates. The simulation of the transmitter (free) diffusion in the vesicle (but also in the pore and the space between the plasma membrane and the electrode) followed methods described previously (Glavinović 1999; Ventriglia 2004). Note that the transmitter molecules bound to the gel are not able to diffuse.

Following the opening of the fusion pore the vesicular interior is in a direct contact with the extracellular fluid. If the catecholamine molecules are bound to the gel matrix, their release may be controlled by a process of ion exchange (Uvnas and Aborg 1989). As a result of the exchange of the fixed charges of such polyionic matrices and the charged moieties in the bathing medium, these matrices may swell and condense. Modeling of release from swellable gel systems is a moving boundary, or Stefan–Newmann diffusion problem (Lee 1980; 1985). The constitutive equation for transport of the releasing substance, in the presence of both diffusional and relaxational phenomena is highly nonlinear, and as a result the exact analytical solutions are not available (Crank 1984). Moreover, the equations required for fitting the swellable systems are quite different from those for non–swellable systems (Ritger and Peppas 1987a; Schroeder et al. 1996). We therefore used the empirical relation for the dissociation from a swellable gel matrix given by Ritger and Peppas (1987b):

$$M_t = K_g t^n, \tag{1}$$

where M_t is the fraction of polymer content released at time t (i.e. a non-dimensional parameter indicating the release ratio at a time t and at infinity), K_g is the dissociation constant and n is the diffusion exponent, which depends on the geometry of the system and is 0.432 ± 0.007 for Fickian diffusion from a swellable sphere.

2.2 Computer simulations

All simulations were done using Matlab. Initially the transmitter molecules, which were either all free or all bound, were distributed uniformly but randomly and their concentration was 500 mM (Winkler et al. 1986; Finnegan et al. 1996; Glavinović et al. 1998). The vesicles whose radii were 40, 60, 80 and 100 nm thus had 80,720, 272,429, 645,757 and 1,261,240 molecules, respectively. The dissociation of the transmitter molecules bound to the gel follows Eq.(1) and is a random process. There is no binding of free transmitter molecules to the gel. If the transmitter is bound to the gel, the dissociation constant of the gel matrix will largely determine the transmitter release kinetics (see Sect. 3). Because no direct evidence exists as to what this constant should be,

we examined the 'parameter space' (i.e. we evaluated how the transmitter release, cleft processes and amperometric currents are affected with changes of the dissociation constants over a wide range of values – two orders of magnitude). Even if the dissociation constant lies beyond the values examined, the variables of interest can be inferred given the trends, which are clear (see Sect. 3). The dissociation is considered to be fast if $K_g = 1.0$, medium if $K_g = 0.1$ and slow if $K_g = 0.01$. The diffusion of free catecholamine molecules was modeled as a random walk. The length traveled by a catecholamine molecule (in each of three dimensions) is chosen randomly from a Gaussian distribution with mean of 0 and a standard deviation σ given by

$$\sigma = \sqrt{2D\delta t}, \quad (2)$$

where the δt is the length of the time step and D is the diffusion coefficient of the transmitter molecule. Diffusion coefficient of catecholamines ranged from $0.75 \cdot 10^{-6}$ to $6.0 \cdot 10^{-6}\,\mathrm{cm^2/s}$. In the vesicle, and the space between the secretory cell and the recording electrode (cleft), the transmitter molecules collide elastically with the "walls" of the space, whenever they hit or cross the walls. Collisions are considered elastic if their velocity components parallel to the surface are conserved (in sign and in amplitude), whilst the normal velocity component maintains the amplitude, but changes the sign. Once the transmitter molecules leave the cleft they are removed from the system i.e. they cannot return to the cleft.

Since the time resolution of spontaneous current spikes is ~1–100 μs, we choose 0.2 μs time steps for diffusion (Wahl et al. 1996; Glavinović 1999). Because of the small pore diameter and this choice of the time step, the calculations of the particle trajectories (including multiple reflections) in the fusion pore have to be done using additional constraints (note that having a smaller time step would render the simulations very slow owing to the typically very large number of transmitter molecules which have to be followed). Once the molecules entered into the pore their x and y positions were set to zero, and the release becomes a release from a point source in the middle of the pore. The time course of release should not be affected by these changes, because the movements in three directions (x, y and z) are independent, and given that the pore diameter is very small, there should be only marginal changes of the spatial distribution of molecules in the cleft or of their chance of being consumed and when. This was nevertheless tested further. Firstly, we chose the values of the fixed x and y positions other than (0,0), and secondly we released the molecules from the fusion pore spatially uniformly, instead as a point source (in both cases the time course of release remained the same). The spatial distribution of molecules in the cleft, the amplitude and the time course of the 'recorded' currents were not visibly changed (not shown), validating the choice of the time step and the approach used in simulations.

Whenever the molecule hits the electrode surface, a random number, between 0.0 and 1.0, is chosen from a uniform distribution. If this random number is less than a predetermined fractional number P, the molecule is presumed to have reacted with the electrode, and as a result of oxidation two electrons are generated (Schroeder et al. 1996). If the random number is between P and 1.0, the elastic reflection is assumed to occur and the molecule continues to move. Assuming $P = 1$ (i.e. 100% electrode efficiency) is equivalent to assuming a zero concentration at the surface of electrode as a boundary condition, when partial differential equations are used to solve this diffusion problem (and is assumed in some, but not all, of our simulations). If no consumption at the electrode surface occurs $P = 0$, and the electrode acts as a simple diffusion barrier. Finally $P = 0.1$ indicates 10% electrode efficiency. Choosing $0 < P < 1$ is appropriate if the electrode reaction (and thus the electrode efficiency) is for whatever reason (such as polarization) reduced. The vesicular diameters ranged from 80 to 200 nm, the fusion pore length was set at 15 nm whilst the radius was either 2.5 or 5 nm (Khanin et al. 1994; Glavinović 1999; Ventriglia 2004). The cleft width ranged from 100 nm to 1.0 μm and the electrode dimensions were 2 μm × 2 μm, and thus for the widest cleft the distance between the locus of release and the end of the cleft is exactly the same as the cleft width.

The amplitudes, rise times and decay times of the free vesicular transmitter concentrations, of the cleft and pore-mouth concentrations, and of the amperometric currents were determined from the best fits. The fitting equation was in all cases: $y = A \cdot \exp^{-a \cdot t} \cdot (1 - \exp^{-b \cdot t})$, where t was time and y was either the free vesicular, cleft or pore-mouth concentration or the amperometric current.

3 Results

3.1 Effect of fusion pore diameter and speed of transmitter dissociation from gel on vesicular transmitter concentration

The amplitude and the time course of the free vesicular transmitter concentration strongly depend on the fusion pore diameter, which was set at either 5 nm (Fig. 1a,b) or 10 nm (Fig. 1c,d). Given the initial transmitter concentration of 500 mM and the diameter of 120 nm, the vesicle initially contained 272, 429 molecules. The length of the fusion pore was 15 nm, and the cleft width and length were 100 nm and 2 μm, respectively (see Sect. 2). The speed of transmitter dissociation from the gel matrix influences the amplitude and the rise phase of the free vesicular concentration, but appears to have little effect on its decay phase (Fig. 1a–d). The dissociation is considered to be fast if $K_g = 1.0$, medium if $K_g = 0.1$ and slow if $K_g = 0.01$ (see Sect. 2). Finally, the diffusion constant of the transmitter in the vesicle and fusion pore also affects the time course of free transmitter (Fig. 1a,c). The diffusion constant was $6.0 \cdot 10^{-6}\,\mathrm{cm^2/s}$ in all simulations except in Fig. 1a,c, where lower diffusion constant ($0.75 \cdot 10^{-6}\,\mathrm{cm^2/s}$) was also used (dashed and dotted lines), in which case there was no gel in the vesicle (i.e. all transmitter molecules were free initially).

It may be argued that the depletion of the vesicular transmitter near the entrance of the fusion pore may be another

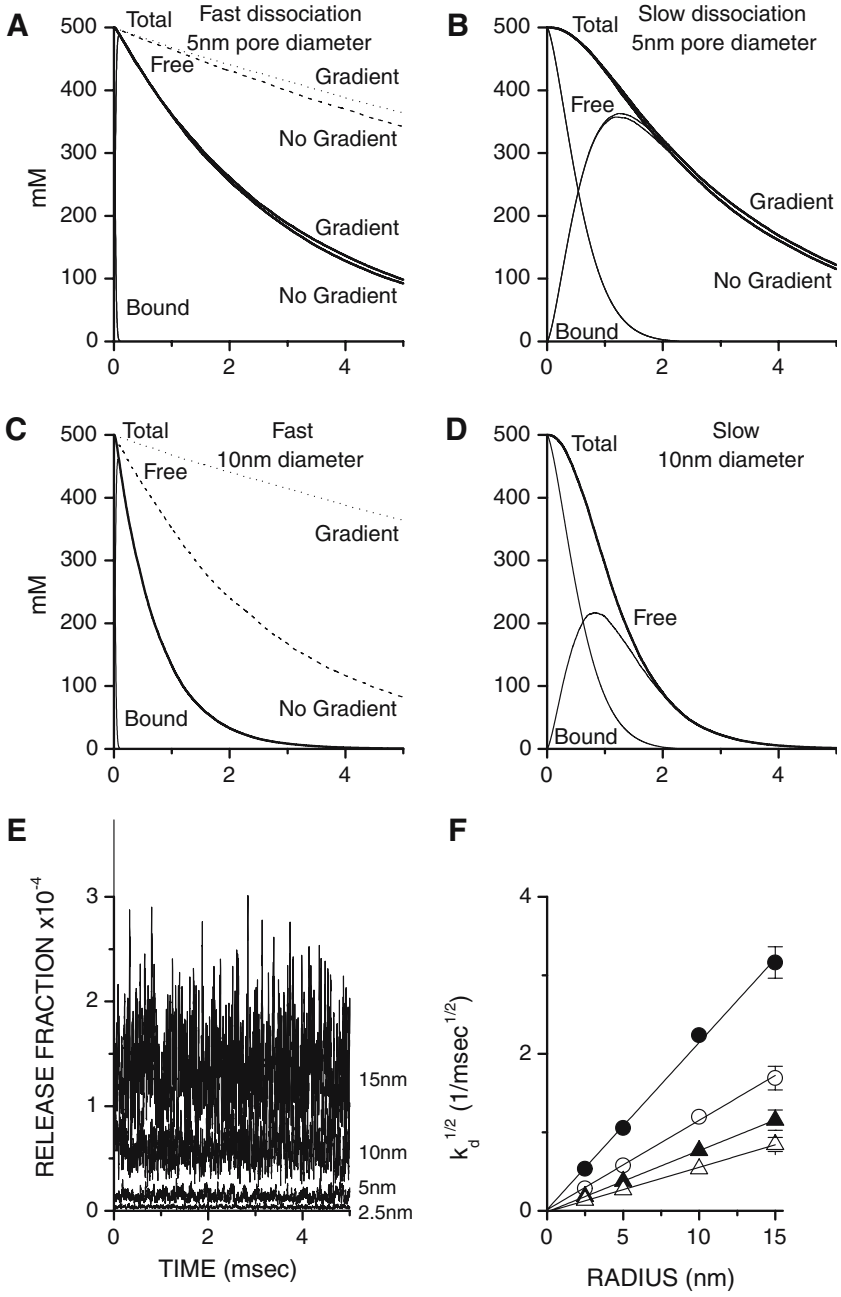

Fig. 1 Time course of the vesicular transmitter concentration – total (*thick line*), gel bound (*thin line*) and free (*medium line*). The transmitter dissociation from the gel matrix, which was either fast (**a, c**) or slow (**b, d**; see text) affects the time course of the change in free and bound transmitter concentrations. The concentration changes more rapidly if the fusion pore diameter is larger, whilst lowering the diffusion constant in the vesicle and fusion pore from $6.0 \cdot 10^{-6}$ to $0.75 \cdot 10^{-6}$ cm^2/s slows time course of free transmitter (*dotted lines*). To evaluate how the development of the transmitter concentration gradient near the entrance to the fusion pore affects the free vesicular concentration (and release), the molecular positions within the vesicle were randomized at each simulation step (**a**–**c**). Abolishing the concentration gradient speeds-up but only marginally the time course of the free transmitter if the diffusion constant is the same as in aqueous solution (i.e. $6.0 \cdot 10^{-6}$ cm^2/s). The speeding-up is more pronounced if the diffusion constant is lower ($0.75 \cdot 10^{-6}$ cm^2/s; **a**, **c**) and especially when the fusion pore diameter is wide (10 nm; **c**). **e** Release fraction (estimated as the ratio of the number of molecules released to the number of free molecules in the vesicle) remains constant as the vesicle empties, but rises as the fusion pore radius increases. **f** The square root of the rate of decay of release is linearly related to the fusion pore radius, but the slope of the relationship is greater for smaller vesicles. Symbols give averages of three estimates. The averaging time window was 1.0 m. Vertical bars are standard errors, and are given only for the estimates whose radius is maximal to avoid crowding. There was no randomization to abolish the concentration gradient in the vesicle and the diffusion constant was $6.0 \cdot 10^{-6}$ cm^2/s (**e, f**).

important factor limiting the release, and thus increasing the amplitude of the free transmitter and slowing its time course, but this was clearly not the case. To assess its importance we ran some simulations that were in all respects identical, but whereby at each simulation step the location of all free transmitter molecules in the vesicle was randomized. If the concentration gradient is eliminated throughout the vesicle at each time step the amplitude and the time course of the free transmitter remained the same (Fig. 1a,e; see also Fig. 1b,f).

Lack of concentration gradient near the entrance to the fusion pore argues that the release fraction of vesicular content (defined as the number of molecules released at any time relative to the total number of all free molecules in the vesicle) will remain constant during release and that it will be determined by 'geometric factors'. This was indeed the case. The release fraction was constant over time for a wide range of fusion pore radii (2.5–15 nm; Fig. 1e; the simulation conditions were as in Fig. 1a). If the geometric factors (i.e. the vesicular and fusion pore radii) govern the release of transmitter the decay rate should be proportional to the ratio of the cross-sectional fusion pore to vesicular surface areas, and the $k_d^{1/2}$ versus r_{fp} relationship should be linear. k_d was the decay time of transmitter release and r_{fp} the fusion pore radius. This was indeed the case over a wide range of fusion pore radii and for vesicular radii ranging from 40 to 100 nm (Fig. 1f). The lines, estimated using the least-square fitting method were: $k_d^{1/2} = 0.02 + 0.21 \cdot r_{fp}$ (40 nm radius vesicle; filled circles); $k_d^{1/2} = 0.01 + 0.11 \cdot r_{fp}$ (60 nm radius vesicle; empty circles); $k_d^{1/2} = -0.01 + 0.08 \cdot r_{fp}$ (80 nm radius vesicle; filled triangles); $k_d^{1/2} = -0.02 + 0.06 \cdot r_{fp}$ (100 nm radius vesicle; empty triangles).

Figure 2 summarizes how much the fusion pore radius and the speed of dissociation of the transmitter from the gel matrix alter the relationship between the 'true' quantal size (defined as the number of molecules initially present in the vesicle) and the peak amplitude, rise time or decay time of the vesicular free transmitter concentration. Note that such a definition assumes a complete release of the vesicular content, which may not always be the case. The rise time was defined as the time interval needed for the free transmitter concentration to reach from 10 to 90% of the maximal value, and the decay time as the time interval needed for the free transmitter concentration to decay from the maximum to 1/e of the maximum. Figure 2a shows the concentration peak amplitude versus 'true' quantal size relationship. Increasing the fusion pore radius and slowing the transmitter dissociation lowers the concentration amplitude, and the effect is especially pronounced for smaller vesicles. The rise times are long when the dissociation from the gel is slow, but are shortened if the fusion pore radius increases. The rise times are longer for larger vesicles, but only if the dissociation from the gel is slow (Fig. 2b). Large vesicles have much longer decay times especially if the fusion pore radii are small, but are un-affected by the speed of dissociation from the gel. The relationships are completely overlapping in the absence of the vesicular concentration gradient (triangle down semi-black; Fig. 2c), but also if the release occurs into the infinite space (not shown). In the absence of the gel matrix the amplitude of the free transmitter concentration is equal to the initial concentration, the rise time is infinitely short (i.e. both are independent of the diffusion constant of the transmitter in the vesicle and fusion pore), whilst the decay time of the free concentration strongly depends on the diffusion constant.

3.2 Changing electrolysis efficiency alters cleft transmitter concentration but current amplitude and its time course are largely unchanged

The transmitter accumulations averaged over the whole cleft during amperometric recording are small. They rise as the efficiency diminishes [from maximal (100%) to one tenth of the maximal (10%) value], but the concentration remains low (Fig. 3a). The cleft width was 100 nm, as may be encountered during amperometric recordings (Walker et al. 1996; Westerink et al. 2000). The vesicular radius was 40 nm in both cases, and given the initial total vesicular concentration of 500 mM the number of transmitter molecules (all bound initially) was 80,720. The maximal concentration in the cleft at the mouth of the fusion pore (defined as the small volume centered in the middle of the cleft where the transmitter is released, with a 50 nm radius and spanning the whole cleft width, which was set to 100 nm) was higher but still far below (< 2 mM) the vesicular concentration of free transmitter, even when the electrode efficiency was low (10%; Fig. 3b,c). The pore-mouth concentration was generally independent of the electrode efficiency, the vesicular (and thus the quantal) size, or the speed of transmitter dissociation from the gel matrix (Fig. 3f,g). The cleft concentration, which was generally much lower, changed as the electrode efficiency changed, but only if the cleft was narrow (Fig. 3d,e). It can thus be safely concluded that there is no cleft-to-vesicle feedback during amperometric recordings.

The presence of the electrode and its consumption level do not appear to alter the current amplitude or its time course. Figure 4a and b shows two currents, one simulated assuming a maximal (i.e. 100%) electrolysis, and another assuming a much lower – 10% electrolysis level. Note large fluctuations of the simulated currents. In both cases, the vesicular radius was 40 nm and the cleft width 100 nm, the initial vesicular concentration was 500 mM, the number of transmitter molecules – all bound initially – was 80,720, whilst the speed of the transmitter dissociation from the gel matrix was medium (see Sect. 2). Indeed the amplitude, rise and decay times are largely independent of the electrolysis level, for both narrow and wide clefts (Fig. 4c–h). However, the current amplitudes and their time course were modified by other factors. The rise time was shortened as electrode efficiency rose, but only moderately and only if the cleft was narrow. The rise time strongly depended on the speed of the transmitter dissociation from the gel matrix, especially if the cleft was narrow. In contrast the vesicular size determined the decay time. These influences were examined in detail (see Sect. 3.3).

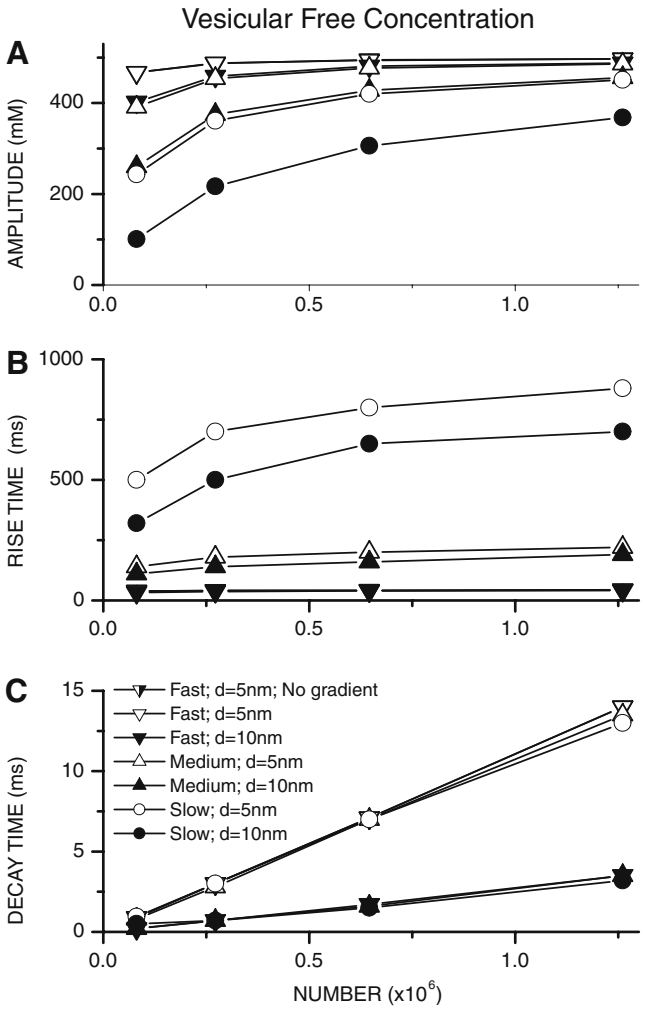

Fig. 2 a Vesicular free transmitter concentration versus quantal size relationship is steeper for slower transmitter dissociation from the gel matrix and when fusion pore radii are larger. The number of transmitter molecules initially present in the vesicle (abscissa) gives the quantal size (see text). **b** Slower transmitter dissociation also renders the vesicular concentration rise time versus quantal size relationship steeper, which is further increased if the fusion pore radius is small. **c** Vesicular concentration decay time versus quantal size relationship is very steep especially if the fusion pore radii are small, but are unaffected by the speed of dissociation from the gel. Randomization of the transmitter molecules, which prevents the development of the intra-vesicular concentration gradient, did not alter the amplitude, rise time or decay time versus quantal size relationships, which were completely overlapping. Symbols give averages of three estimates. Vertical bars, which are standard errors, are all too small to be visible

3.3 Transmitter Escapes as Cleft Widens

Figure 5a and b shows the time course of transmitter release and its consumption by the electrode. Figure 5c depicts the integrals of the number of transmitter molecules, which escaped from the cleft, those released and those consumed together with the time course of the number of transmitter molecules in the cleft. Given a comparatively wide cleft it is not surprising that the rise time of the number of transmitter molecules consumed is slower than that of the number released. The general similarity of the amplitude and the decay time was more surprising. A 500 nm cleft is considered wide because the width is comparable to the distance between the release site and the edge of the cleft. The vesicular radius was 40 nm (which yields 80,720 molecules given the initial concentration of 500 mM), the radius of the fusion pore was 2.5 nm, the cleft was $2\,\mu\text{m} \times 2\,\mu\text{m} \times 500\,\text{nm}$, and the electrode efficiency was 100%.

The fraction of the transmitter molecules that escapes from the cleft rises as the cleft widens. Increasing the electrode efficiency tenfold (from 10 to 100%) reduced the escape fraction especially when the cleft is narrow (Fig. 5f). The greater escape fraction with wider clefts does not reduce the current amplitude directly, because very few molecules escape during the rise time. Nevertheless fewer molecules are consumed in such cases (lowering the current amplitude) and many eventually escape during the decay phase. Note also that the effect of the wider cleft (and greater escape fraction) on the decay phase is similarly complex. On the one hand the progressively greater escape fraction during the decay phase tends to shorten the decay time, but the longer transmitter dwell time observed in such cases lengthens it. Finally note that: (a) the maximal cleft concentration versus cleft width relationship is not linear but shows a broad maximum (Fig. 5d), and (b) the maximal cleft number versus cleft width relationship, though positive is sub-linear (Fig. 5e). This was further explored.

3.4 Spatio-temporal distribution of transmitter in the cleft

Knowledge of the changes of the pore-mouth and overall cleft concentrations and of the transmitter escape, that occur as cleft width or electrode efficiency change provides only a partial insight into the role of cleft processes in determining the amperometric currents. The transversal (across the cleft) and lateral (along the cleft) changes of the transmitter concentration provide additional understanding. The spatio-temporal distribution of the transmitter (or of any diffusible substance) in the constricted space is known, if there is no chemical reaction, and if the release occurs from an instantaneous point source (Crank, 1984). However, it is less clear what the distribution should be if the release is not instantaneous, and if there is an electro-chemical reaction such as electrolysis. Figure 6b shows a tri-dimensional snapshot of the transmitter molecules in the cleft 100 μs from the start of release from a vesicle. The geometry of the secretion is depicted in the schematic diagram (approximately to scale) shown in Fig. 6a. The vesicular radius was 60 nm, the fusion pore radius and length were 2.5 and 15 nm, respectively, and the cleft dimensions were $2\,\mu\text{m} \times 2\,\mu\text{m} \times 100\,\text{nm}$.

The cleft concentration may be lower near the electrode surface both because the transmitter is ‘consumed’ by the electrode, and because of transmitter released from the vesicle (on the other side). The electrode consumption clearly lowers the cleft concentration near the electrode surface when the cleft is narrow. Figure 6c and e depicts two cases, one at

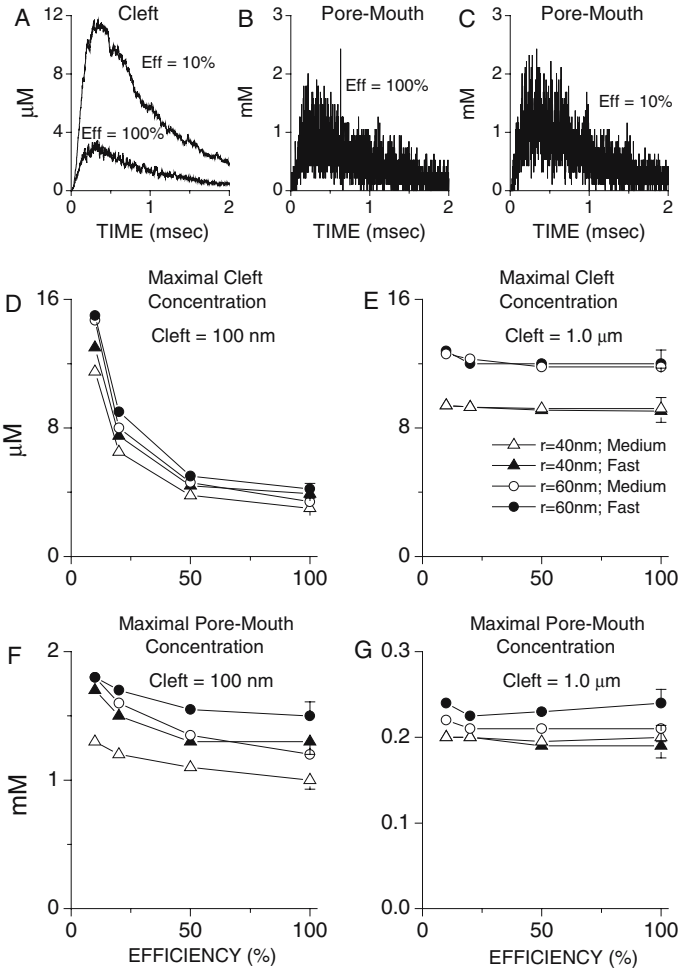

Fig. 3 Drastic reduction of the efficiency of the electrolysis level produces a marked rise of the transmitter concentration in the cleft if the cleft is narrow, but produces no change if the cleft is wide. **a** The transmitter concentration in the cleft for two extreme efficiency levels (10 and 100%). **b** and **c** The transmitter concentration at the mouth of the fusion pore (see text), for low and high efficiency levels, are very similar. **d** and **e** Maximal cleft concentration diminishes as the electrode efficiency rises, if the cleft is narrow, but remains un-altered if the cleft is wide. **f** and **g** In contrast, the maximal pore mouth transmitter concentration is essentially independent of the electrode efficiency for both narrow and wide clefts. Symbols give averages of three estimates; vertical bars are standard errors

100% and another at 10% electrolysis level. If the cleft is wide the transversal concentration gradient is much greater, but the gradient is almost entirely due to the transmitter influx from the vesicle, and is not altered by the varying electrode efficiency (Fig. 6d,f). The zero distance indicates the electrode surface, whilst the 0.1 or 1.0 distances represent the location of the plasma membrane. The lateral spread is curtailed by the electrode consumption when the cleft is narrow, though not greatly (Fig. 6g,i), but not when it is wide (Fig. 6h,j). The zero distance indicates the center of the cleft whilst the 1.0 distance represents the end of the cleft. The combined effect of the cleft width, and the electrode efficiency in controlling the lateral spread, is summarized in Fig. 6k and l. The median radius (defined as the radius, where half of the transmitter molecules are inside, and other half outside) increases as the cleft width rises, and the increase is evident at 0.1 and 2 ms from the start of release, and for two extreme values of the electrode efficiency (10 and 100%). The time course of the rise of the median radius is rapid. Moreover it reaches a plateau in less than 1 ms (Fig. 6l). The median radius is not affected by the variations of the electrode efficiency if the cleft is wide. However, for a narrow cleft the time to reach the plateau is shorter and the plateau level is higher.

3.5 Amplitude and time course of amperometric currents is strongly affected by the cleft width

The experimental evidence and the theoretical analysis have shown that the current amplitudes diminish as the cleft width rises whilst the rise and decay times lengthen (Wightman et al. 1991). Although the theoretical conclusions do not differ from the experimental findings the question requires a re-evaluation to elucidate how changes of the electrode

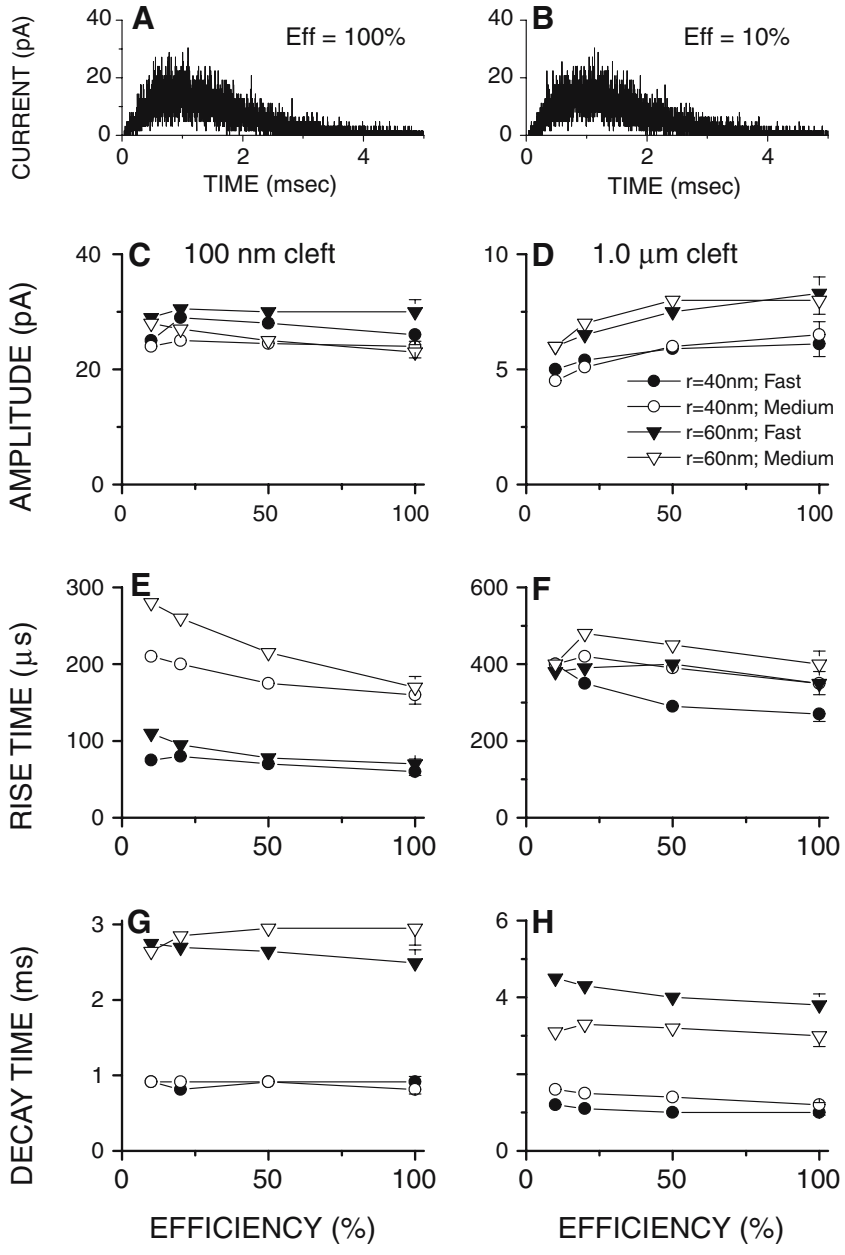

Fig. 4 Even a drastic change of the efficiency of the electrolysis level altered the current amplitude or its time course only modestly, irrespective of whether the cleft width was narrow or wide, or whether the time course of release was fast or slow. The release kinetics were altered by varying the speed of the transmitter dissociation from the gel matrix, but also by changing the vesicular size. **a** and **b** Two current traces, for two extreme efficiency values are shown (as indicated). The amplitude versus electrode efficiency (**c, d**), the rise time versus electrode efficiency (**e, f**) and the decay time versus electrode efficiency relationships (**g**, **h**). Symbols give averages of three estimates. Vertical bars are standard errors

efficiency alter such dependence. Fig. 7a–c shows three current 'traces' simulated assuming three different cleft widths (as indicated). The vesicular radius was 60 nm, whilst the fusion pore radius and length were 2.5 nm and 15 nm respectively. The current amplitudes are smaller and the rise times slower with wider clefts, but the decay time does not appear to be affected. This was examined in detail. As Fig. 7d–f shows, as the cleft widened, the peak current amplitude diminished, the rise time lengthened, but the decay time remained essentially the same. Changing the vesicular size or the speed of the transmitter dissociation from the gel matrix did not alter the amplitude versus cleft width relationship significantly. However, the rise-time versus cleft width relationship was steeper with slower transmitter dissociation from the gel matrix. In contrast the speed of dissociation had essentially no effect on the decay time versus cleft width relationship. The vesicular size did not alter the slope of the relationship but the decay time was clearly longer for larger vesicles. The vesicular

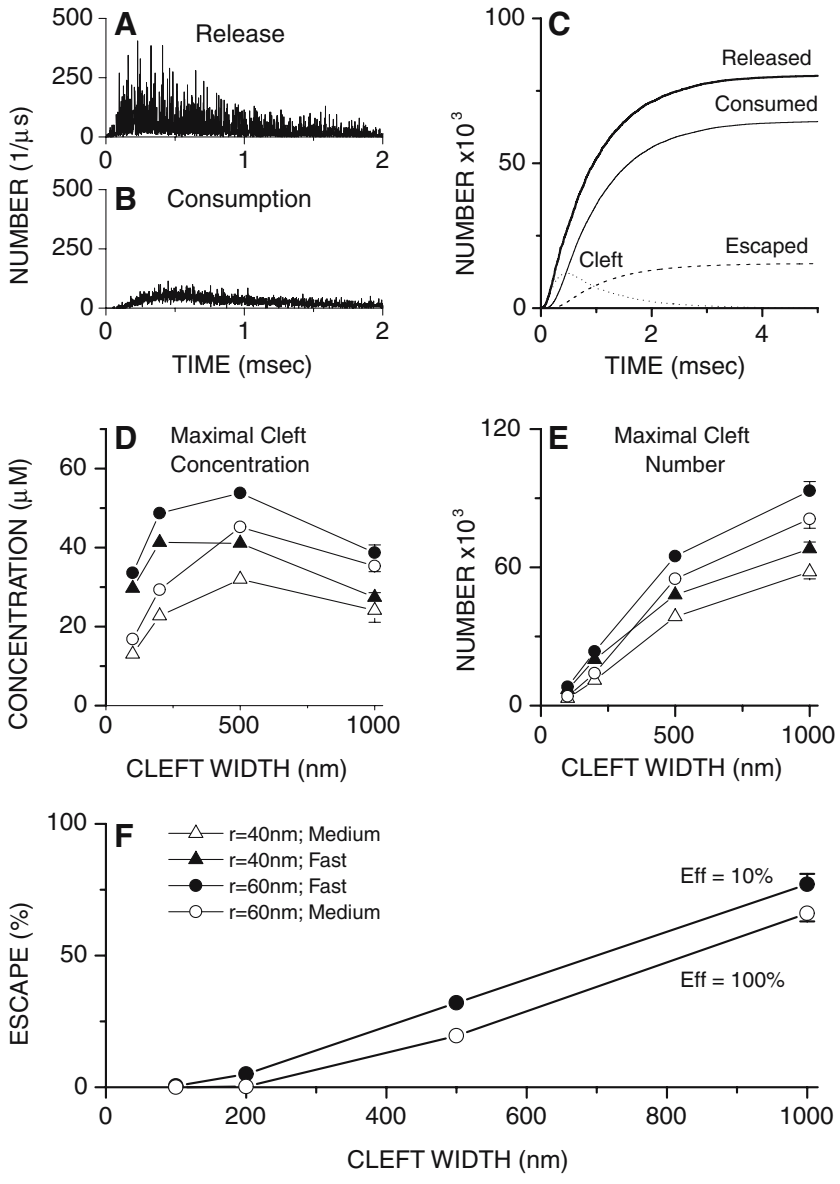

Fig. 5 The fraction of transmitter molecules escaping from the cleft can be an important factor affecting the current amplitude and its time course. **a** and **b** The number of molecules consumed by the electrode has a slower rise time and is more noisy but its amplitude and the decay time are similar to the number of molecules released. **c** The cumulative time course of the number of transmitter released is below that of the transmitter consumed due to the significant fraction of the transmitter, which escaped. The time course of the change in number of transmitter molecules in the cleft is shown for comparison. **d** The maximal transmitter concentration in the cleft versus cleft width relationship is not linear but shows a broad maximum. **e** The maximal number of transmitter molecules in the cleft versus cleft width relationship is positive but sub-linear. **f** The fraction of the transmitter molecules, which escapes from the cleft, is large when the cleft is wide. High electrode efficiency reduces this fraction but only modestly for wide clefts. Symbols give averages of three estimates. Vertical bars are standard errors

radius was either 40 or 60 nm (as indicated) and the fusion pore radius was 2.5 nm. The transmitter dissociation from the gel matrix was either fast or medium (see Sect. 2).

3.6 Relationship between quantal sizes, amplitudes, rise and decay times of recorded currents

The evaluation of the relationships among the parameters describing the amperometric currents can be useful for analysis of what the kinetics of release of vesicular content are and how they are governed by the speed of the transmitter dissociation from gel matrix or the fusion pore diameter. The amplitude versus quantal size relationship is not steep if the transmitter dissociation from gel matrix is fast, but becomes so if the dissociation is slow, especially if the fusion pore radius is large. Interestingly, cleft widening also alters the relationship, making it steeper (Fig. 8a,b). The rise-time and the decay-time versus quantal size relationships are influenced by the same factors though differently (Fig. 8c–f). The rise-time versus quantal size relationship is steep only when

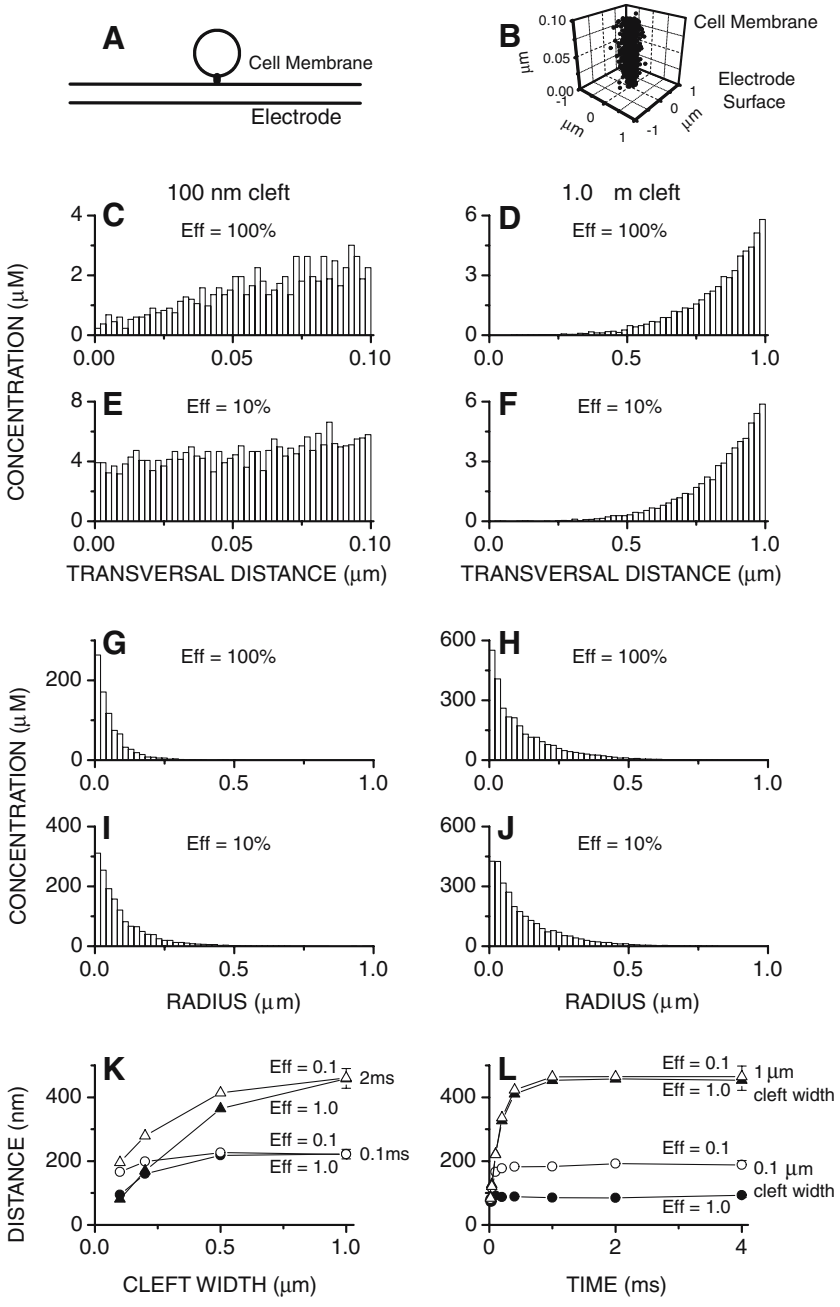

Fig. 6 **a** Schematic diagram (approximately to scale) of the vesicle connected through the fusion pore to the plasma membrane, and releasing its contents into the cleft (i.e. the space separating the secretory cell and the carbon electrode). **b** Tri-dimensional snapshot of the transmitter molecules in the cleft 100 μs from the start of release from a vesicle. **c–f** The transmitter concentration in the cleft versus axial distance. **g–j** The transmitter concentration in the cleft versus radial distance. When the cleft is narrow greater electrode efficiency reduces the concentration throughout the cleft, but especially near the electrode surface (**c–f**), and the spatial spread of transmitter is curtailed (**g–j**). **k** The median spatial spread increases as the cleft width rises and is evident at 0.1 and 2 ms from the start of release and simulation and for two extreme electrode efficiencies. **l** Rapid rise of the median spatial spread is observed even for a wide cleft, but is followed by a plateau. Whilst the plateau levels are essentially the same for two extreme cases of electrode efficiency when the cleft is wide the levels differ significantly for a narrow cleft. Symbols give averages of three estimates. Vertical bars are standard errors

the transmitter dissociation is slow. In contrast the decay-time vs. quantal size relationship is generally steep, but especially so if the fusion pore radius is small. The speed of transmitter dissociation and the cleft width do not alter it significantly. Finally, note that lowering the diffusion constant in the cleft from $6.0 \cdot 10^{-6}$ cm^2/s to $0.75 \cdot 10^{-6}$ cm^2/s does not lead to a great prolongation of the time course, but either to a marginal prolongation of the rise times (Fig 8c), or a moderate shortening of the decay times (Fig. 8e). Small amplitude reduction is also observed (Fig. 8a).

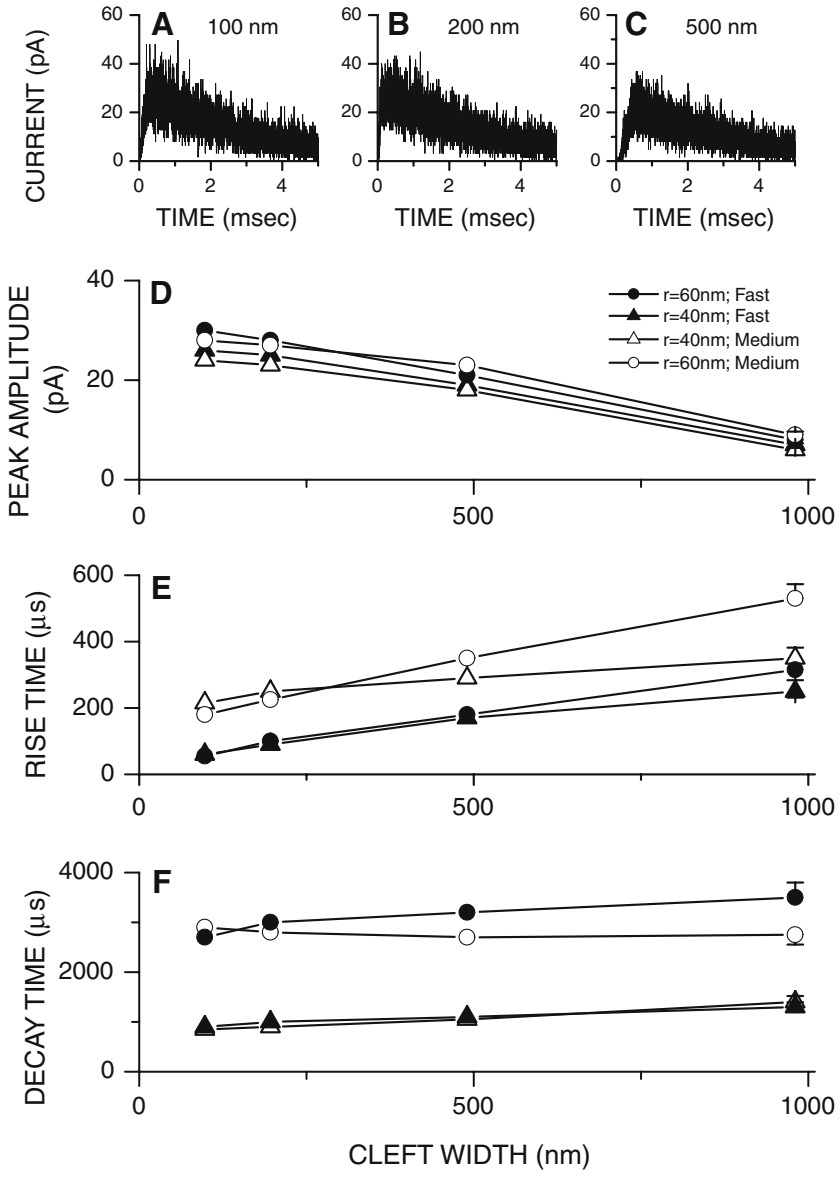

Fig. 7 The amperometric current amplitude diminishes whilst its time course slows when the cleft widens. **a**-**c** Three simulated current traces for three different cleft widths (as indicated) are shown. **d** The peak current diminishes when the cleft width rises, but is largely independent of either the speed of transmitter dissociation from the gel matrix or the vesicular size. **e** The rise time is longer when the cleft is wider, but is also influenced by both the vesicle size and the speed of the transmitter dissociation from the gel matrix. **f** The prolongation of the decay time is modest when the cleft widens. The decay time is also largely independent of the speed of the transmitter dissociation from the gel matrix, but its duration is longer for larger vesicles. Symbols give averages of three estimates, whilst vertical bars are standard errors

Figure 9a–d shows the amplitude (A) dependence of the rise times (τ_rs), and decay times (τ_ds) for different fusion pore radii, transmitter dissociation speeds and cleft widths. The equivalent rise time versus decay time relationship are shown in Fig. 9e and f. Finally, Table 1. summarizes how the speed of the transmitter dissociation from the gel matrix, the fusion pore radius and the cleft width alter the slope of the $\tau_r - A$ and $\tau_d - A$ relationships. Briefly, as the speed of the transmitter dissociation from the gel matrix rises the slope of the $\tau_r - A$ relationship diminishes. The effect on the $\tau_d - A$ relationship is less clear and both an increase and a decrease are observed. However, as the fusion pore radius increases and the release becomes faster, both the $\tau_r - A$ and $\tau_d - A$ relationships become less steep, irrespective of the speed of transmitter dissociation. Finally, as the cleft widens both $\tau_r - A$ and $\tau_d - A$ relationships become steeper.

3.7 Direct comparison of released, cleft and consumed transmitter

Our analysis so far has demonstrated that the time course of release closely corresponds to the time course of the

Table 1 Slopes of the best fitting lines to the data pairs of the decay times (τ_d), or rise times (τ_r) on the one hand, and amplitudes (A) on the other, and their correlation coefficients (R)

	Fast		Medium		Slow	
	Slope (ms/pA)	R	Slope (ms/pA)	R	Slope (ms/pA)	R
$R_{pore} = 2.5$ nm $D_x = 100$ nm						
$\tau_r : A$	0.01 ± 0.01	0.34	0.02 ± 0.01	0.86	0.03 ± 0.01	0.97
$\tau_d : A$	1.44 ± 1.10	0.68	1.53 ± 0.79	0.81	0.84 ± 0.35	0.86
$R_{pore} = 5.0$ nm $D_x = 100$ nm						
$\tau_r : A$	0.00 ± 0.00	0.69	0.00 ± 0.00	0.99	0.01 ± 0.00	0.99
$\tau_d : A$	0.19 ± 0.05	0.93	23.5 ± 20.4	0.63	0.04 ± 0.02	0.85
$R_{pore} = 2.5$ nm $D_x = 1{,}000$ nm						
$\tau_r : A$	0.05 ± 0.01	0.97	0.05 ± 0.03	0.81	0.15 ± 0.04	0.92
$\tau_d : A$	4.39 ± 2.22	0.81	2.31 ± 0.73	0.91	2.03 ± 0.97	0.83
$R_{pore} = 5.0$ nm $D_x = 1{,}000$ nm						
$\tau_r : A$	0.01 ± 0.00	0.99	0.01 ± 0.00	0.99	0.02 ± 0.00	0.97
$\tau_d : A$	0.11 ± 0.00	0.90	0.11 ± 0.03	0.94	0.12 ± 0.05	0.89

vesicular free transmitter concentration. Moreover, changes in neither the electrode efficiency (even when large) nor cleft width have a profound effect on the decay time of amperometric current suggesting that, after initial equilibration in the cleft, the time course of the current closely resembles the time course of the cleft concentration as well as that of the release. This was tested directly. After an early equilibration in the cleft, the ratio of the number of consumed and released transmitter molecules during quantal event is constant, for a narrow and wide cleft (Fig 10a,b). Similar time independence is observed for the ratio of the number of transmitter molecules consumed by the electrode and those in the cleft (Fig 10c).

4 Discussion

4.1 Vesicular transmitter and its time course of release

As stated in the Introduction the transmitter in neuro-endocrine cells appears to be stored in an osmotically inactive form on a gel matrix. What is less clear is whether the slow time course of the amperometric currents is due to the slow dimerization of the transmitter from the gel matrix, low diffusion constant of transmitter (in the vesicle, fusion pore or the cleft), or large vesicular size (Wightman et al. 1991; Walker et al. 1996; Westerink et al. 2000; Gil et al. 2001; Hafez et al. 2005). In this study we evaluated using Monte Carlo simulations (Wahl et al. 1996; Glavinović 1999; Bennett et al. 2004) how the speed of dissociation of a transmitter from the gel matrix, as well as the fusion pore and vesicular size, influence the time course of transmitter in the vesicle. Let us assume a simple model of storage and release, with the release fraction being the same for all free molecules of transmitter, and governed by the ratio of the fusion pore to vesicular surface area. Such a model implies a rapid equilibration of vesicular transmitter concentration. Whether the equilibration is rapid or whether a concentration gradient develops during the release was tested directly by comparing the transmitter concentrations with and without randomization of transmitter positions. Randomization procedure completely eliminates any gradients. When the diffusion constant of transmitter was the same in the vesicle as in the cleft (i.e. $6.0 \cdot 10^{-6}$ cm^2/s) the time course was identical in both cases, demonstrating that there was no concentration gradient. How fast the vesicular free transmitter concentration and release are, is then largely determined by the vesicular geometry, which governs the release over its entire time course, but also by the speed of dissociation of the transmitter from the gel matrix, which, however, influences mainly the amplitude and the rise phase. Note that the fusion pore is assumed to be either open or closed. If the pore initially opens gradually, or if its diameter changes during the decay time, such dynamic changes of the pore size would alter the time course of release significantly, given a very strong dependence of the release on the fusion pore diameter. However, in neuro-endocrine cells even large changes of the quantal size appear not to be associated with the changes of the fusion pore diameter (Kebir et al., 2005).

When the diffusion constant in the vesicle was reduced the randomized and non-randomized time courses were different. The intra-vesicular concentration gradient thus developed and reduced the availability of some transmitter molecules for release. The availability of transmitter molecules for release appears to be reduced (either by binding of transmitter to the gel matrix, or due to lower diffusion constant in the vesicle, or through some other mechanism). In the absence of such a mechanism the process of release of vesicular content would be a Poissonian process. The variance of its fluctuations would be very high (the variance is equal to the mean in a Poissonian process), contrary to what amperometric recordings show (Finnegan et al. 1996; Glavinović et al. 1998; Anderson et al. 1999).

Cleft processes do not significantly affect the release of vesicular content (i.e. there is no 'cleft to vesicle feedback') because the transmitter concentration in the cleft at the mouth

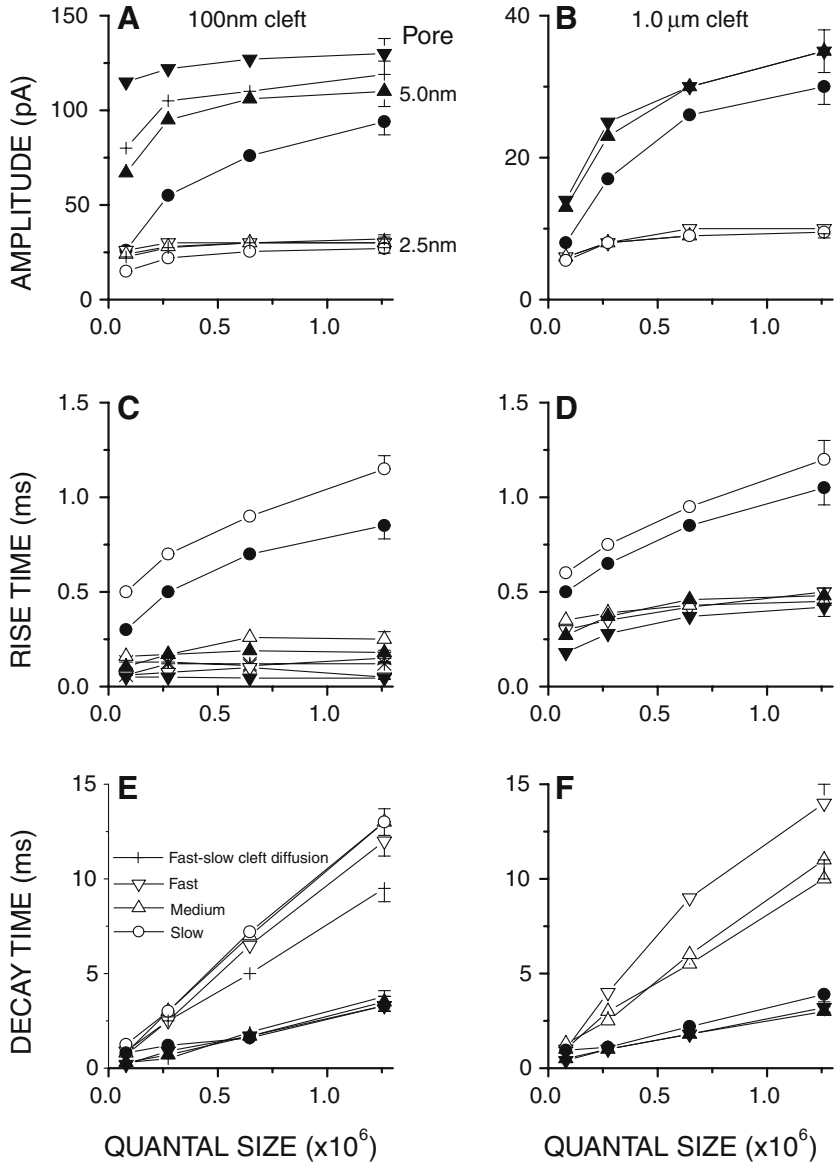

Fig. 8 The quantal size dependence of the amperometric current amplitudes (**a**, **b**), the rise times (**c**, **d**) and the decay times (**e**, **f**) depends on the cleft width, the speed of the transmitter dissociation from the gel matrix and the fusion pore radius, which was either 2.5 nm (*empty symbols*) or 5 nm (*filled symbols*). The diffusion constant in the vesicle and fusion pore was $6.0 \cdot 10^{-6}$ cm^2/s. Same constant was used in the cleft except in two cases where a lower value ($0.75 \cdot 10^{-6}$ cm^2/s) was also used (*cross symbols*: **a**, **c** and **e**). Note that a low diffusion constant in the cleft leads to a small amplitude and decay time reduction. The number of molecules initially present in the vesicle is the quantal size. *Symbols* give averages of three estimates. *Vertical bars* are standard errors

of the fusion pore is, as a rule, much lower than the vesicular concentration. Indeed the time course of vesicular free concentration in such a recording mode is almost identical to the time course estimated when the release occurs into an open space constrained only by the presence of the secretory cell. This is not surprising. Under conditions of a release into a semi-infinite space the transmitter concentration diminishes to a very low level a short distance from the release site, because of the semi-infinity of the space, and in the amperometric mode because of the concentration clamp enforced by the recording electrode.

4.2 Electrode efficiency does not affect amperometric currents but may change cleft transmitter concentration

The most surprising finding of the present simulations is that the amplitude and time course of amperometric currents changed very little, even when the electrolysis level changed tenfold, and irrespective of whether the cleft was narrow or wide. This finding however, can be understood by considering: (a) the effects of the electrolysis on the transmitter concentration in the cleft, first near its entry and then throughout the cleft, and (b) an interplay between the transmitter

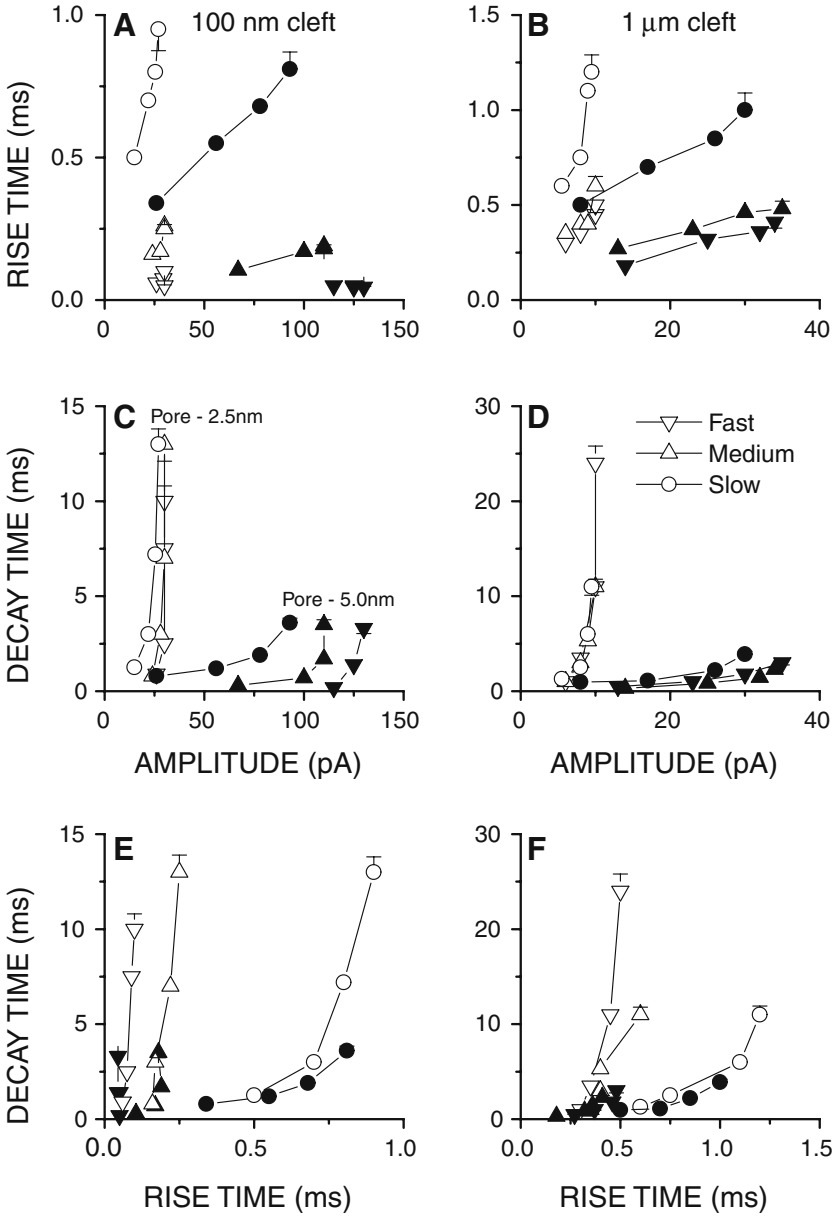

Fig. 9 The amplitude dependence of the amperometric current rise times (**a**, **b**), and decay times (**c**, **d**) varies with the cleft width, fusion pore radius and the transmitter dissociation from the gel matrix. The rise time versus decay time relationship is also influenced by the same factors. The fusion pore radius was either 2.5 nm (*empty symbols*) or 5 nm (*filled symbols*). *Symbols* give averages of three estimates, and *vertical bars* are corresponding standard errors

diffusion and its consumption by the electrode. Given a diffusion constant of catecholamine of 600 μm^2/s (see Sect. 2) the mean diffusion length is 73.4 nm for 10 μs time interval; 100 nm is traversed on average in 18.6 μs. The transversal equilibration thus occurs very quickly if the cleft is narrow (i.e. if the recording electrode is positioned ~100 nm from the plasma membrane). The transmitter spreads further laterally, but more interestingly an 'apparent' though slower lateral equilibration is also eventually observed. In the absence of transmitter consumption by the electrode (i.e. with restricted diffusion source and open boundaries alone) the lateral equilibration does not exist, but the electrode consumption eventually curtails the lateral spread and establishes an apparent equilibrium.

Given rapid diffusion it is not surprising that the transmitter concentration in the cleft at the mouth of the fusion pore is essentially independent of the electrode efficiency over a wide range of efficiencies and cleft widths. The balance between the equilibration and the electrode consumption favors such an outcome. Both, the 'influx' of the transmitter from the fusion pore, and its 'efflux' into the cleft space further away are much greater than the consumption by the electrode, even when the consumption is maximal.

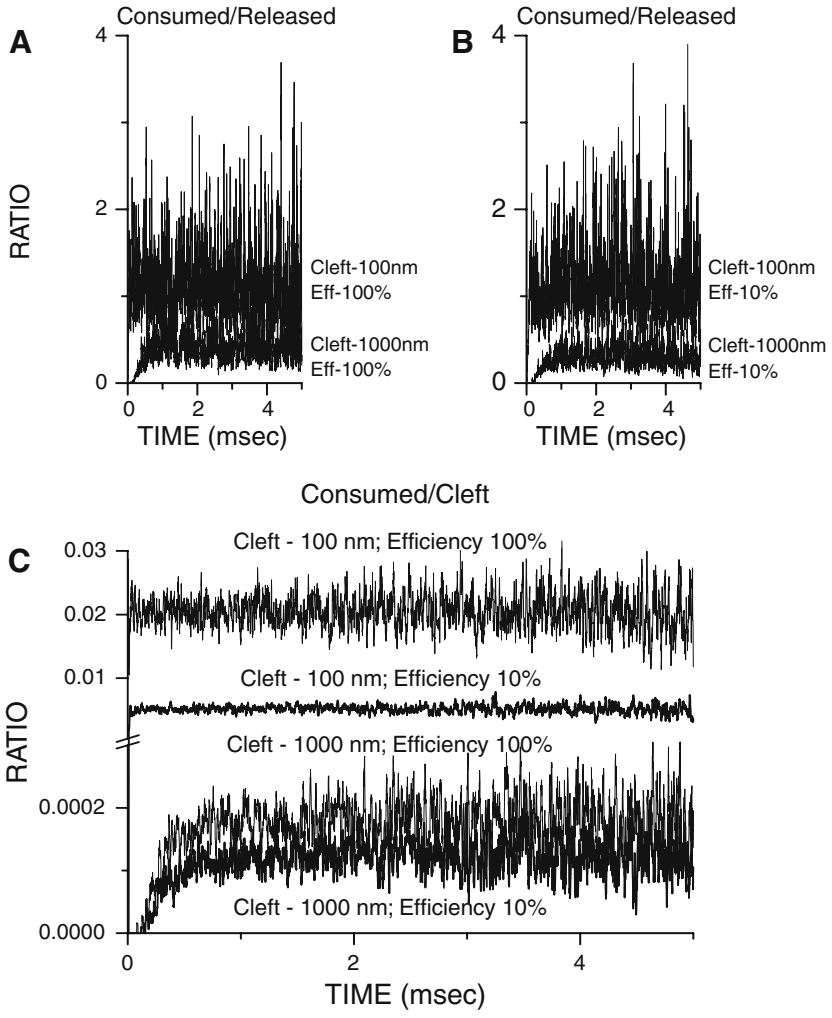

Fig. 10 **a** and **b** The ratio of the number of electrode consumed to released transmitter molecules is constant during a quantal event for a narrow cleft, but also for a wide cleft following the early equilibration in the cleft. **c** Similar time independence is observed for the ratio of the number of transmitter molecules consumed to those in the cleft

The electrode efficiency becomes important in lowering the cleft concentration where the influx, efflux (and thus the transmitter concentration) are low, but only if the cleft is narrow. As electrolysis is reduced the transmitter molecules linger longer in the cleft, but the additional time is very short (a few microseconds). The time course of both the transmitter concentration in the cleft, and the recorded current remain thus essentially intact, but the amplitude of the cleft concentration rises, because the cleft dwell time (the time a molecule spends in the cleft before being consumed) is very short and even a prolongation of few microseconds leads to a significantly greater total dwell time. As the nearly constant current amplitude indicates, the direct effect of lower electrolysis (lower transmitter consumption) is almost balanced by the indirect effect (greater transmitter cleft concentration). Though the increase is less pronounced overall, it is greater near the electrode surface, and the molecules near the electrode surface have a higher probability of being consumed. Finally, the electrolysis not only lowers the overall cleft concentration, it also effectively curtails the lateral spread of the transmitter.

If the cleft is wide the dwell time of molecules is generally longer (especially of those far from the electrode surface), but the relative prolongation of the dwell time, due to the lower electrolysis, is smaller. Even near the electrode surface the electrolysis has very little effect on the concentration, because the molecules are quickly replenished by those further away. Consequently, the change of the electrolysis level has very little effect on the current amplitude or its time course. In conclusion, any change of the electrode efficiency that may occur experimentally (due to a change of the holding potential or the electrode resistance), may alter significantly the optical recordings of the catecholamine transients in the cleft (Terakawa et al. 1995; Tsuboi et al. 2002), but will leave the amperometric recordings essentially intact. Finally note that the insensitivity of the recorded currents to even pronounced changes of the electrode efficiency, may have important implications for the use of cyclic voltametry,

in detecting various transmitters when the detection volume is very small and diffusion highly restricted.

4.3 Effect of release kinetics, cleft width and transmitter diffusion constant in the cleft on amplitude dependence of rise and decay times of amperometric currents

The amplitude dependence of the rise and decay times of the amperometric currents can be used as a potentially important source of information about the mechanism of release as it may help determine how much the speed of transmitter dissociation from the gel matrix, vesicular and fusion pore geometry and cleft processes influence the time course of release. The analysis revealed that the steepness of the $A - \tau_d$ and $A - \tau_r$ relationships was strongly influenced by the release kinetics, irrespective of whether kinetics was altered by the changing ratio of the fusion pore and vesicular radii, or the speed of transmitter dissociation from the gel matrix, becoming steeper with slower release kinetics. The reasons however were different. Slower transmitter dissociation caused steeper $A - \tau_r$ relationship by enhancing τ_r variability, and smaller fusion pore radius by reducing the amplitude variability. The speed of the transmitter dissociation did not affect either τ_d or $A - \tau_d$ relationship, but smaller fusion pore radius reduced the amplitude variability and increased the τ_d variability thus rendering the $A - \tau_d$ relationship steeper. Finally, it is necessary to stress that it is not only the kinetics of release of the vesicular content, but also the cleft width that determined how steep the $A - \tau_d$ and $A - \tau_r$ relationships were. This may appear surprising but it is simply due to the fact that the amplitudes became less variable with wider cleft.

Recent evidence argues that the effective diffusion constant in the cleft near the membrane of the secreting chromaffin cells is considerably lower than in aqueous solution, due to reversible binding of transmitter molecules to the cell membrane. It was thus suggested that it is not slow release kinetics, due to the slow dissociation from the granule matrix, but slow diffusion in the cleft that renders the amperometric currents recorded near the cell surface slow (Hafez et al., 2005). The diffusion constant is likely to be lower in confined spaces and the reversible binding of transmitter molecules to the vesicular and pore membrane (which given the geometry should be even more pronounced) should render the release kinetics slow. We evaluated whether lowering the diffusion constant from $6.0 \cdot 10^{-6}$ to $0.75 \cdot 10^{-6}\,cm^2/s$ slows amperometric currents, but this was not the case. Whilst the rise times increased marginally the decay times either remained the same or were shortened modestly. While this may appear surprising it should be kept in mind that, though a lower diffusion constant slows diffusion of transmitter, it also reduces its spatial spread in the cleft.

Finally note that when the transmitter dissociation from the gel matrix was fast the parameters describing the amperometric currents (the rise time, the amplitude and the decay time) were in several important respects incompatible with experimental findings (Schroeder et al. 1994; Walker et al. 1996; Amatore et al. 2000; Tang et al. 2005). The long decay times observed experimentally could occur only if the diameters of the fusion pores were very small, but in such a case: (a) the amplitudes would be essentially independent of the quantal size (i.e. the number of molecules in the vesicle), and (b) the rise times would be too short and essentially determined by the transmitter equilibration in the cleft. The simulations thus demonstrate that the kinetics of catecholamine release is slow probably due to the slow transmitter dissociation from the gel matrix.

Acknowledgements This work was supported by the grants from the Heart and Stroke Foundation of Canada and Canadian Institutes of Health Research to M.I.G. Dr. K. Krnjevic and Dr. J. Winslow read the manuscript and made valuable comments.

References

Amatore C, Bouret Y, Travis ER, Wightman RM (2000) Interplay between membrane dynamics, diffusion and swelling pressure governs individual vesicular exocytotic events during release of adrenaline by chromaffin cells. Biochimie 82:481–496

Anderson BB, Zerby SE, Ewing AG (1999) Calculations of transmitter concentration in individual PC12 cell vesicles with electrochemical data and a distribution of vesicle size obtained by electron microscopy. J Neurosci Methods 88:163–170

Aspinwall CA, Brooks SA, Kennedy RT, Lakey JRT (1997) Effects of intravesicular H^+ and extracellular H^+ and Zn^{2+} on insulin secretion in pancreatic beta cells. J Biol Chem 272:31308–31314

Bennett MR, Farnell L, Gibson WG (2004) The facilitated probability of quantal secretion within an array of calcium channels of an active zone at the amphibian neuromuscular junction. Biophys J 86:2674–2690

Brozoski TJ, Brown RM, Rosvold HE, Goldman PS (1979) Cognitive deficit caused by regional depletion of dopamine in prefrontal cortex of rhesus monkey. Science 205:929–932

Coupland RE (1968) Determining sizes and distribution of sizes of spherical bodies such as chromaffin granules in tissue sections. Nature 217:384–388

Crank J (1984) Free and moving boundary problems. Clarendon Press, Oxford, UK

Di Chiara G, Bassareo V, Fenu S, De Luca MA, Spina L, Cadoni C, Acquas E, Carboni E, Valentini V, Lecca D (2004) Dopamine and drug addiction: the nucleus accumbens shell connection. Neuropharmacol 47:227–241

Eccles JC, Jaeger JC (1958) The relationship between the mode of operation and the dimensions of the junctional regions at synapses and motor end-organs. Proc Royal Soc B 148:38–56

Finnegan JM, Pihel K, Cahill PS, Huang L, Zerby SE, Ewing AG,Kennedy RT, Wightman RM (1996) Vesicular Quantal Size Measured by Amperometry at Chromaffin, Mast, Pheochromocytoma, and Pancreatic-Cells. J Neurochem 66:1914–1923

Frucht SJ (2004) Parkinson disease: an update. Neurologist 10:185–194

Garris PA, Ciolkowski EL, Pastore P, Wightman RM (1994) Efflux of dopamine from the synaptic cleft in the nucleus accumbens of the rat brain. J Neurosci 14:6084–6093

Gil A, Viniegra S, Gutierrez LM (2001) Temperature and PMA affect different phases of exocytosis in bovine chromaffin cells. Eur J Neurosci 13:1380–1386

Glavinović MI (1999) Monte Carlo simulation of vesicular release, spatio-temporal distribution of glutamate in synaptic cleft, and generation of postsynaptic currents. Pflugers Archiv Eur J Physiol 437:462–470

Glavinović MI, Rabie HR (1997) Monte Carlo simulation of release of content of individual vesicles in secretory cells. Abstr Soc Neurosci 23:366

Glavinović MI, Vitale ML, Trifaro JM (1998) Comparison of vesicular volume and quantal size in bovine chromaffin cells. Neuroscience 85:957–968
Hafez I, Kisler K, Berberian K, Dernick G, Valero V, Yong MG, Craighead HG, Lindau M (2005) Electrochemical imaging of fusion pore openings by electrochemical detector arrays. Proc Natl Acad Sci USA 102:13879–13884
Jena BP, Cho SJ, Jeremic A, Stromer MH, Hamdah RA (2003) Structure and composition of the fusion pore. Biophys J 84:1337–1343
Karunanithi S, Marin L, Wong K, Atwood HL (2002) Quantal size and variation determined by vesicle size in normal and mutant Drosophila glutamatergic synapses. J Neurosci 22:10267–10276
Kebir S, Aristizabal F, Maysinger D, Glavinović MI (2005) Rapid change of quantal size in PC-12 cells detected by neural networks. J Neurosci Methods 142:231–242
Kelly RB (1993) Storage and release of neurotransmitters. Cell 72:45–53
Khanin R, Parnas H, Segel L (1994) Diffusion cannot govern the discharge of neurotransmitter in fast synapses. Biophys J 67:966–972
Lee PI (1980) Diffusion release of a solute from a polymeric matrix: approximate analytical solutions. J Membr Sci 7:255–275
Lee PI (1985) Kinetics of drug release from hydrogel matrices. J Contr Rel 2:277–288
Monck JR, Fernandez JM (1992) The exocytotic fusion pore. J Cell Biol 119:1395–1404
Ritger PL, Peppas NA (1987a) A simple equation for description of solute release. I. Fickian and non-Fickian release from non-swellable devices in the form of slabs, spheres, cylinders or discs. J Contr Rel 5:23–36
Ritger PL, Peppas NA (1987b) A simple equation for description of solute release. I. Fickian and anomalous release from swellable devices. J Contr Rel 5:37–42
Saulle E, Centonze D, Martin AB, Moratalla R, Bernardi G, Calabresi P (2002) Endogenenous dopamine amplifies ischemic long-term potentiation via D1 receptors. Stroke 33:2978–2984
Schikorski T, Stevens CF (1997) Quantitative, ultrastructural analysis of hippocampal excitatory synapses. J Neurosci 17:5858–5867
Schroeder TJ, Jankowski JA, Senyshyn J, Holz, RW, Wightman RM (1994) Zones of exocytotic release on bovine adrenal medullary cells in culture. J Biol Chem 269:17215–17220
Schroeder TJ, Borges R, Finnegan JM, Pihel K, Amatore C, Wightman RM (1996) Temporally resolved, independent stages of individual exocytotic secretion events. Biophys J 70:1061–1068
Spruce AE, Breckenridge LJ, Lee AK, Almers W (1990) Properties of the fusion pore that forms during exocytosis of a mast cell secretory vesicle. Neuron 4:643–654
Sulzer D, Pothos EN (2000) Regulation of quantal size by presynaptic mechanisms. Rev Neurosci 11:159–212
Tanaka S (2005) Dopaminergic control of working memory and its relevance to schizophrenia: a circuit dynamics perspective. Neuroscience (in press). DOI:10.1016/J.neuroscience.20 05.08.070
Tang KS, Tse A, Tse FW (2005) Differential regulation of multiple populations of granules in rat adrenal chromaffin cells by culture duration and cyclic AMP. J Neurochem 92:1126–1139
Terakawa S, Kumakura K, Duchen M (1995) Spatiotemporal analysis of quantal secretory events from bovine adrenal chromaffin cells in culture. J Physiol (Lond) 487:59–60
Tsuboi T, Kikuta T, Sakurai T, Terakawa S (2002) Water secretion associated with exocytosis in endocrine cells revealed by micro forcemetry and evanescent wave microscopy. Biophys J 83:172–183
Uvnas B, Aborg CH (1989) Role of ion exchange in release of biogenic amines. News Physiol Sci 4:68–71
Ventriglia F (2004) Saturation in excitatory synapses of hippocampus investigated by computer simulations. Biol Cybern 90:349–359
Wahl LM, Pouzat C, Stratford KJ (1996) Monte Carlo Simulation of fast excitatory synaptic transmission at a hippocampal synapse. J Neurophysiol 75:597–608
Walker A, Glavinović MI, Trifaro JM (1996) Time course of release of content of single vesicles in bovine chromaffin cells. Pflugers Archiv Eur J Physiol 431:729–735
Westerink, RHS, de Groot A, Vijverberg HPM (2000) Heterogeneity of catecholamine-containing vesicles in PC12 cells. Biochem Biophys Res Comm 270:625–630
Wightman RM, Jankowski JA, Kennedy RT, Kawagoe KT, Schroeder TJ, Leszczyszyn DJ, Near JA, Diliberto EJ, Viveros OH (1991) Temporally resolved catecholamine spikes correspond to single vesicle release from individual chromaffin cells. Proc Natl acad Sci USA 88:10754–10758
Winkler H, Apps DK, Fischer-Colbrie R (1986) The molecular function of adrenal chromaffin granules: established facts and unresolved topics. Neuroscience 18:261–290
Yoo SH, Lewis MS (1993) Dimerization and tetramerization properties of the C-terminal region of chromogranin A: a thermodynamic analysis. Biochemistry 32:8816–8219